Urea-Induced Sequential Unfolding of Fibronectin: A Fluorescence Spectroscopy and Circular Dichroism Study

Salima Patel,[‡] Alain F. Chaffotte,[§] Fabrice Goubard,[||] and Emmanuel Pauthe*[,‡]

ERRMECE, Université de Cergy-Pontoise, 95302 Cergy-Pontoise Cedex, France, LPPI, Université de Cergy-Pontoise, 95301 Cergy-Pontoise Cedex, France, and Institut Pasteur, 28 rue du Dr. Roux, Paris, France

Received May 2, 2003; Revised Manuscript Received December 10, 2003

ABSTRACT: Fibronectin (FN) is an extracellular matrix (ECM) protein found soluble in corporal fluids or as an insoluble fibrillar component incorporated in the ECM. This phenomenon implicates structural changes that expose FN binding sites and activate the protein to promote intermolecular interactions with other FN. We have investigated, using fluorescence and circular dichroism spectroscopy, the unfolding process of human fibronectin induced by urea in different ionic strength conditions. At any ionic strength, the equilibrium unfolding data are well described by a four-state equilibrium model $N \leftrightarrows I_1 \leftrightarrows I_2 \leftrightarrows U$. Fitting this model to experimental values, we have determined the free energy change for the different steps. We found that the $N \leftrightarrows I_1$ transition corresponds to a free energy of 10.5 ± 0.4 kcal/mol. Comparable values of free energy change are generally associated with a partial unfolding of the type III domain. For the $I_1 \leftrightarrows I_2$ transition, the free energy change is 7.6 ± 0.4 kcal/mol at low ionic strength but is twice as low at high ionic strength. This result is consistent with observations indicating that the complete unfolding of the type III domain from partially unfolded forms necessitates about 5 kcal/mol. The third step, $I_2 \leftrightarrows U$, which leads to the complete unfolding of fibronectin, corresponds to a free energy change of 14.4 ± 0.9 kcal/mol at low ionic strength whereas this energy is again twice as low under high ionic strength conditions. This hierarchical unfolding of fibronectin, as well as the stability of the different intermediates controlled by ionic strength demonstrated here, could be important for the understanding of activation of the matrix assembly.

Fibronectin is a multifunctional glycoprotein expressed by various cell types (hepatocytes, fibroblasts, macrophages, and leucocytes, among others). This protein, circulating in the blood and plasma, could be transformed by cultured fibroblasts into an insoluble fibrillar component of the extracellular matrix (ECM)[1] (*1*). Once incorporated, fibronectin becomes a prominent constituent of ECM around and beneath many cells. It provides substrates for cell adhesion and migration during development, wound healing, and other situations, as well as affecting many cellular functions including proliferation, survival, and differentiation (*2*, *3*).

This large glycoprotein is a dimer. The two subunits of around 250 kDa are covalently linked via two disulfide bonds near their carboxy termini. Each subunit is composed of a series of modular domains known as fibronectin repeats I, II, and III (12, 2, and 15 copies, respectively). Modules of type I, II, and III consist of about 45, 60, and 90 amino acids, respectively. The 12 type I modules are disposed as follows: 9 make up the NH_2 terminus and 3 end the COOH terminus of the polypeptide (*4*). Two type II modules interrupt a row of nine type I modules. Fifteen type III modules make up the middle of the polypeptide. Type I, II, and III modules are also found in many other proteins, type III even being ubiquitous in animal protein (*5*). They are connected by short polypeptide segments sensitive to proteinases and are regrouped in functional domains that express specific binding activities (*6*). X-ray crystallography and NMR spectroscopy have been successfully used to elucidate the structure of some individual modules or short fragments. Their structure was found as being mainly β-sheet, and the three types of modules are considered as globular (*7*, *8*).

Under plasmatic buffer conditions (10 mM Tris-HCl, 150 mM NaCl, pH 7.4), at room temperature, the conformation of the whole fibronectin has been investigated by several techniques. Among recent works, it has been showed that under such buffer conditions fibronectin conformation implies both large-scale flexibility and local order. Results from light scattering and small angle neutron scattering have shown that the native fibronectin conformation is consistent with a Gaussian chain of 56 globular modules (*9*). Concerning the secondary structure, it has been unambiguously established that native fibronectin contains about 43% β-sheet, 28% turns, and 25% unordered structures (*10*, *11*).

However, though conformation and structure of whole fibronectin in well-defined solution have been precisely characterized, studies concerning fibronectin stability and/or structural behavior in various conditions have been

* To whom correspondence should be addressed. Phone: (33) 1 34 25 66 01. Fax: (33) 1 34 25 65 52. E-mail: emmanuel.pauthe@bio.u-cergy.fr.

[‡] ERRMECE, Université de Cergy-Pontoise.

[§] Institut Pasteur.

[||] LPPI, Université de Cergy-Pontoise.

[1] Abbreviations: ECM, extracellular matrix; FN, fibronectin; FNI, fibronectin domain type I module; FNII, fibronectin domain type II module; FNIII, fibronectin domain type III module; KI, potassium iodide.

10.1021/bi0347104 CCC: $27.50 © 2004 American Chemical Society
Published on Web 01/21/2004

principally restricted to its fragments. Indeed, there are few techniques available to follow structural variations in nonglobular proteins of such high molecular mass. Such studies have been essentially made on type III modules. It is well accepted that there are binding sites hidden in the folded core of FNIII modules, such as the two synergetic sequences, RGD and PSHRN, found in the tenth and the ninth type III module, respectively, and responsible of fibronectin interaction with specific cellular receptors (integrin). Upon a mechanical stretching, these modules could be partially unfolded and become "activated". Exposure of these cryptic sites by mechanical unfolding triggers the binding of FNIII modules from other molecules, favoring matrix assembly (*12*−*14*). Spectroscopic methods and scanning calorimetry have been used to confirm this property of FNIII modules and, in particular, the ninth type III module. It has been clearly demonstrated that temperature-induced unfolding of $FNIII_9$ proceeds through a partially unfolded intermediate which undergoes rapid self-association, leading to the formation of large stable multimers that retain substantial amounts of β-sheet structure (*15*). Such structural organizations might play a role in the regulation of matrix assembly. Furthermore, recent steered molecular dynamics (SMD) simulations have been used to study how mechanical stretching of $FNIII_{9-10}$ affects the relative distance between the RGD and the PHSRN synergetic sequence in $FNIII_{10}$ and $FNIII_9$ modules, respectively. These simulations predict the existence of an intermediate unfolding state in which the synergy−RGD distance is strongly increased and becomes too large to allow both sites to cobind the same receptor. Thus, these simulations suggest that increased $\alpha_5\beta_1$ binding attributed to the synergy site can be turned off mechanically by stretching $FNIII_{9-10}$ into this intermediate state (*16*).

The existence of such intermediate unfolded states could so play a role in the regulation of interactions between matrix proteins (as fibronectin) or between these last ones and other molecules such as the integrin receptors.

Concerning the whole fibronectin, few studies have been realized on the structural variations and stability induced by physical or chemical parameters (such as temperature, pH, or denaturant reagent). Structural modifications of fibronectin induced by increasing temperature have been recently reported, using Fourier transform infrared (FT-IR) and light scattering spectroscopy (*11*). The authors observed that, at high temperature, a partially unfolded state of fibronectin is induced and an aggregation process occurs via the formation of intermolecular hydrogen bonds and intermolecular β-structure. Moreover, effects of ionic strength and pH on fibronectin structure have been investigated by several spectroscopic methods (fluorescence, circular dichroism, etc.). The results suggested that a change in pH or in ionic strength (above 1 M NaCl) induces an unfolding resulting in two loosely associated disk-shaped subunits (*17*). This structural arrangement permits the independent rotational motion of each fibronectin subunit around the carboxyl-terminal interchain disulfide bonds. This conformational change is presumably mediated by the salt- or pH-induced disruption of intersubunit salt bridges and/or hydrogen bonds.

So, these studies concerning structural modifications of fibronectin have been essentially led on electrostatic interactions but not on hydrogen bond interactions which maintain secondary and tertiary structures.

No systematic study of denaturant-induced structural modifications of the whole fibronectin has been reported. In the present work, we analyze the equilibrium urea-induced unfolding of fibronectin under different ionic strength conditions in order to characterize structural changes of fibronectin. Spectroscopic probes, such as fluorescence and circular dichroism, have been used to follow changes in secondary and tertiary structures. Whatever the ionic strength was, the data are well described by the four-state sequential model: $N \leftrightarrow I_1 \leftrightarrow I_2 \leftrightarrow U$. In all cases, the first intermediate I_1 seems to have the same secondary structure content. However, some variations appear in the tertiary structure organization at high ionic strength. Moreover, the stability of intermediates depends on ionic strength.

Effects of ionic strength on the urea-induced denaturation of fibronectin are discussed in terms of stability and structural modifications of the different states. Possible biological implications of intermediate states are discussed in the light of fibril formation and interaction with cellular receptors.

MATERIALS AND METHODS

Fibronectin Purification. Fibronectin was purified from human cryoprecipitated plasma according to a protocol developed in our laboratory that yields a large quantity of homogeneous protein (*18*). This protocol is based on fibronectin affinities for both gelatin and heparin. Briefly, it consists of three liquid chromatography steps: a gelatin affinity followed by a heparin affinity and finally another gelatin affinity chromatography. All chromatography gels were purchased from Chisso Corp., Japan. The purity of the preparation was determined by densitometry analysis of silver nitrate-stained SDS−polyacrylamide gel electrophoresis, 98.2 ± 0.8% (w/w). Fibronectin concentrations were determined by optical absorbance measurements at 280 nm: $A^{1\%} = 12.8$.

Reagents. Ultrapure urea was purchased from Merck. Ultrapure reagent grade tris(hydroxymethyl)aminomethane and sodium chloride were obtained from Research Organics.

Ionic Strength Conditions Used. Denaturation experiments of fibronectin were realized under five different ionic strength conditions: "pure water" at pH 7.4, 1 mM Tris-HCl, pH 7.4, 10 mM Tris-HCl, pH 7.4, and 10 mM Tris-HCl, pH 7.4, containing either 30 or 150 mM NaCl. The ionic strength chosen for the five different buffers is based on the κ_0^{-1} value. This physicochemical parameter, called the screening length for electrostatic interactions, gives some information about the distance of inter- and intramolecular electrostatic interactions in solution (*19*). This parameter equals $(4\pi l_b I)^{-1/2}$, where l_b is the Bjerrum length and I the ionic strength. l_b is the distance at which the Coulomb energy between two charges matches the thermal energy kT. This distance is 7.2 Å for pure water at room temperature.

In pure water (water, 18 MΩ), at pH 7.4, κ_0^{-1} is around 360 Å, which is twice the protein size (150 Å), indicating that inter- and intramolecular repulsive interactions in solution are clearly not negligible. Thus, chains do not attract together in pure water. The same situation applies in 1 mM Tris-HCl, pH 7.4, where κ_0^{-1} is around 150 Å, a value close to that of the protein size. Pure water and 1 mM Tris-HCl conditions are thus called "low ionic strength conditions" in the following.

In 10 mM Tris-HCl, pH 7.4, 10 mM Tris-HCl + 30 mM NaCl, pH 7.4, and 10 mM Tris-HCl + 150 mM NaCl, pH

7.4, κ_0^{-1} is 60, 30, and 10 Å, respectively. These values are smaller than the size of fibronectin. Thus, an increase in ionic strength leads to some attenuated electrostatic attractive interactions, also called screening charge. Consequently, the chains can interact together to some extent in solution. These three buffer conditions are called "high ionic strength conditions" below.

Preparation of Denatured Samples. Urea stock solutions (10 M) were prepared in the five different ionic strength conditions. All solutions were prepared freshly for each experiment and filtered (0.22 μm pore size) before use. For denaturation experiments, samples at constant protein concentration and various urea concentrations were prepared by mixing proper amounts of urea from the 10 M stock solution with constant amounts of native fibronectin in the corresponding buffer. The same procedure applied for renaturation experiments, except native fibronectin was replaced by 10 M urea-denatured fibronectin in the specific buffer. In both denaturation and renaturation experiments the samples were incubated at 24 °C for 24 h before measurements. This incubation time has been found optimal to allow the protein to reach the unfolding/refolding equilibrium at any urea concentrations. A 8 h incubation time led to a noncoincidence between the unfolding and refolding curves. This apparent hysteresis was progressively reduced upon increasing the incubation time and totally disappeared when the incubation time was 24 h or more.

Furthermore, each sample, once incubated for 24 h, was checked for any possible aggregation just before fluorescence or circular dichroism measurements. This was achieved by systematically recording the absorption spectrum of all samples between 220 and 340 nm in a 922 Uvikon spectrophotometer. The absence of turbidity between 310 and 340 nm was taken as indicating that no aggregation occurred. Moreover, the absorption spectrum allowed to check the protein concentration in the samples.

A baseline control was realized for each experiment at any ionic strength, with a series of samples containing urea at various concentrations but where the fibronectin was replaced by the equivalent volume of the appropriate buffer.

Fluorescence Measurements. Fluorescence measurements were performed on a Perkin-Elmer spectrofluorometer, model LS 50B, equipped with a data recorder and a temperature-controlled cell holder. The fluorescence spectra were measured at a protein concentration of 0.1 μM with a 1 cm path length cell and at constant temperature (24 °C). Excitation and emission bandwidths were set at 10 and 5 nm, respectively. Intrinsic fluorescence was excited at 295 nm, and the emission spectra were recorded between 310 and 410 nm.

(A) Fluorescence Quenching Experiments. Tryptophan fluorescence quenching induced by iodide (potassium salt from Sigma) was analyzed according to the Stern−Volmer (*20*) and Lehrer (*21*) equations.

The dynamic quenching process can be described by the classical Stern−Volmer relationship:

$$\frac{F_0}{F} = \frac{\tau_0}{\tau} = 1 + k_q\tau_0[Q]$$

where F_0 and τ_0 and F and τ are the fluorescence intensity and the time constant of fluorescence decay, respectively, in the absence and in the presence of the quencher at a given concentration [Q]; k_q is the bimolecular collisional rate constant between the quencher molecules and the tryptophan residues. The product $k_q\tau_0$, called the Stern−Volmer constant (K_q), is analogous to an equilibrium constant. It reflects the fluorophore accessibility and is thus related to the environmental flexibility of the tryptophans.

Since fibronectin contains more than one tryptophan residue, the Lehrer equation was used to determine the tryptophan-accessible fraction to quencher molecules such as iodide.

$$\frac{F_0}{\Delta F} = \left(\sum_{i=1}^{n} \frac{f_i K_i[Q]}{1 + K_i[Q]}\right)^{-1}$$

where F_0 is the fluorescence intensity in the absence of quencher, $\Delta F = F_0 - F$ is fluorescence decrease for a given quencher concentration [Q], $f_i = F_{0i}/F_0$ is the fractional contribution to the total fluorescence F_0 of fluorescence intensity F_{0i} from the ith fluorophore, and K_i is the Stern−Volmer constant of an individual accessible tryptophan residue.

If each fluorophore accessible to the quencher exhibits the same value of K, the equation becomes

$$\frac{F_0}{\Delta F} = \frac{1}{f_a K[Q]} + \frac{1}{f_a}$$

where $f_a = \sum_{i=1}^{n} f_i$ is the maximum fraction of accessible fluorophores. From this equation, a plot of $F_0/\Delta F = f(1/[Q])$ yields a straight line whose extrapolation at $1/[Q] = 0$ gives the value of $1/f_a$ on the axis $F_0/\Delta F$.

If each accessible fluorophore has a different value of K, the Lehrer relationship can be rewritten as

$$\frac{F_0}{\Delta F} = \frac{1 + \sum_{i=1}^{n} K_i[Q] + \sum_{i,j=1}^{n} K_i K_j[Q]^2 + \ldots}{\sum_{i=1}^{n} f_i K_i[Q]\left(1 + \sum_{j=1}^{n} K_j[Q] + \ldots\right)}$$

where i and j correspond to the ith and jth fluorophores.

At low quencher concentrations, this relationship can be reduced to

$$\frac{F_0}{\Delta F} = \frac{1}{\sum_{i=1}^{n} f_i K_i[Q]} + \frac{\sum_{i=1}^{n} K_i}{\sum_{i=1}^{n} K_i f_i}$$

where the reciprocal of $\sum_{i=1}^{n} K_i / \sum_{i=1}^{n} K_i f_i$ can be considered as an effective average of the maximum fraction of accessible fluorophores, $(f_a)_{eff}$, and $\sum_{i=1}^{n} K_i$ as an effective averaged quenching constant, $(K)_{eff}$.

Values of $(f_a)_{eff}$ and $(K)_{eff}$ associated with the accessible fluorophores are obtained from the extrapolated intercept on the $F_0/\Delta F$ axis of the Lehrer plot and the slope at low quencher concentrations, respectively.

(B) Data Analysis of the Denaturation Process of Fibronectin. The unfolding/refolding transition of fibronectin

was quantitatively analyzed according to the four-state sequential model:

$$N \underset{K_1}{\leftrightarrow} I_1 \underset{K_2}{\leftrightarrow} I_2 \underset{K_3}{\leftrightarrow} U$$

in which N and U are the native and unfolded states, I_1 and I_2 are two unfolding intermediates, and K_1, K_2, and K_3 are the dissociation equilibrium constants of the corresponding steps.

If the total molar concentration of polypeptide chains is N_0, then

$$N_0 = [N] + [I_1] + [I_2] + [U] \quad (1)$$

and the molar fraction of each species is defined as in the equations

$$f_n = [N]/[N_0] \quad (2)$$

$$f_{i1} = [I_1]/[N_0] \quad (3)$$

$$f_{i2} = [I_2]/[N_0] \quad (4)$$

$$f_u = [U]/[N_0] \quad (5)$$

with

$$f_n + f_{I1} + f_{I2} + f_U = 1 \quad (6)$$

The equilibrium constants K_1, K_2, and K_3 are related to the molar fraction of each species and to N_0 as follows:

$$K_1 = f_{i1}/f_n \quad (7)$$

$$K_2 = f_{i2}/f_{i1} \quad (8)$$

$$K_3 = f_u/f_{i2} \quad (9)$$

Using eqs 7−9 and substituting in terms of f_u, eq 6 can also be written as

$$f_u\left(\frac{1}{K_1K_2K_3} + \frac{1}{K_2K_3} + \frac{1}{K_3} + 1\right) = 1 \quad (10)$$

Rearranging eq 10, the fraction of each species is obtained as shown in the equations

$$f_n = \frac{1}{1 + K_1 + K_1K_2 + K_1K_2K_3} \quad (11)$$

$$f_{i1} = \frac{K_1}{1 + K_1 + K_1K_2 + K_1K_2K_3} \quad (12)$$

$$f_{i2} = \frac{K_1K_2}{1 + K_1 + K_1K_2 + K_1K_2K_3} \quad (13)$$

$$f_u = \frac{K_1K_2K_3}{1 + K_1 + K_1K_2 + K_1K_2K_3} \quad (14)$$

At a given denaturant concentration, each equilibrium constant is related to the free energy change of the corresponding step:

$$K_1 = \exp(-\Delta G_1/RT) \quad (15)$$

$$K_2 = \exp(-\Delta G_2/RT) \quad (16)$$

$$K_3 = \exp(-\Delta G_3/RT) \quad (17)$$

where R is gas constant (1.987 cal·mol^{-1}·K^{-1}) and T is the temperature in kelvin. We assumed, as generally accepted, that the free energy change for each step in the reaction is linearly dependent upon denaturant concentration (*22*, *23*):

$$\Delta G_1 = \Delta G^\circ_1 - m_1[\text{denaturant}] \quad (18)$$

$$\Delta G_2 = \Delta G^\circ_2 - m_2[\text{denaturant}] \quad (19)$$

$$\Delta G_3 = \Delta G^\circ_3 - m_3[\text{denaturant}] \quad (20)$$

where ΔG°_1, ΔG°_2, and ΔG°_3 are the free energy changes in the absence of denaturant and m_1, m_2, and m_3 are the free energy dependences upon denaturant concentration associated with each step.

From eqs 15−20, the K_1, K_1K_2, and $K_1K_2K_3$ expression can be written as follows:

$$K_1 = \exp\frac{-(\Delta G^\circ_1 - m_1[U])}{RT} \quad (21)$$

$$K_1K_2 = \exp\frac{-[\Delta G^\circ_1 + \Delta G^\circ_2 - (m_1 + m_2)[U]]}{RT} \quad (22)$$

$$K_1K_2K_3 = \exp\frac{-[\Delta G^\circ_1 + \Delta G^\circ_2 + \Delta G^\circ_3 - (m_1 + m_2 + m_3)[U]]}{RT} \quad (23)$$

The amplitude of the spectroscopic signal determined at any denaturant concentration is assumed to be a linear combination of the fractional contribution from each species:

$$Y = Y_N f_n + Y_{I1} f_{I1} + Y_{I2} f_{I2} + Y_U f_U \quad (24)$$

where Y_N, Y_{I1}, Y_{I2}, and Y_U are the specific contributions of each species to the signals.

Using eqs 11−14, eq 24 can be expressed as

$$Y = \frac{Y_N + Y_{I1}K_1 + Y_{I2}K_1K_2 + Y_UK_1K_2K_3}{1 + K_1 + K_1K_2 + K_1K_2K_3} \quad (25)$$

From eqs 21−23, eq 25 can be written as follows:

$$Y = \left\{Y_N + Y_{I1}\exp\left(\frac{-(\Delta G^\circ_1 - m_1[U])}{RT}\right) + Y_{I2}\exp\left(\frac{-(\Delta G^\circ_1 + \Delta G^\circ_2 - (m_1 + m_2)[U])}{RT}\right) + Y_U\exp\left(\frac{-(\Delta G^\circ_1 + \Delta G^\circ_2 + \Delta G^\circ_3 - (m_1 + m_2 + m_3)[U])}{RT}\right)\right\} \Big/ \left\{1 + \exp\left(\frac{-(\Delta G^\circ_1 - m[U])}{RT}\right) + \exp\left(\frac{-(\Delta G^\circ_1 + \Delta G^\circ_2 - (m_1 + m_2)[U])}{RT}\right) + \exp\left(\frac{-(\Delta G^\circ_1 + \Delta G^\circ_2 + \Delta G^\circ_3 - (m_1 + m_2 + m_3)[U])}{RT}\right)\right\} \quad (26)$$

Thus, the final relationship (eq 26) that expresses the observed signal Y as a function of the denaturant concentration, contains 10 unknowns: Y_N, Y_{I1}, Y_{I2}, Y_U, $\Delta G°_1$, $\Delta G°_2$, $\Delta G°_3$, m_1, m_2, and m_3.

(C) Nonlinear Least-Squares Fitting Procedure. The 10 unknown parameters, $\Delta G°_1$, $\Delta G°_2$, $\Delta G°_3$, m_1, m_2, m_3, Y_N, Y_{I1}, Y_{I2}, and Y_U, were deduced from the transition curves at any ionic strength by fitting the data to eq 26, developed in terms of $\Delta G°_1$, $\Delta G°_2$, $\Delta G°_3$, m_1, m_2, and m_3, using the nonlinear least-squares procedure included in the software Fig.P (version 2.7) from Biosoft (Cambridge, U.K.). At each ionic strength, three independent series of data were collected and analyzed. To avoid any divergence during the minimization procedure, the number of unknown parameters was restricted by setting as fixed parameters the specific fluorescence of the native and fully unfolded states, Y_N and Y_U, using the experimental fluorescence values measured at 0 and 10 M urea, respectively. Additionally, at low ionic strength, the specific fluorescence of the first intermediate Y_{I1} was graphically estimated between 3 and 4 M urea and also set as constant during the fitting procedure. In a second fitting step, all of the 10 parameters were set as floating. The robustness of the fit was tested by initializing the fitting session with different sets of initial estimates.

Circular Dichroism Measurements. All CD measurements were acquired with a CD6 spectropolarimeter from Jobin-Yvon. In the far-UV CD, spectra were recorded between 195 and 260 nm with a 0.02 cm path length cell at protein concentrations around 2 μM. Each spectrum results from averaging five successive scans recorded at constant bandpass (2 nm) with a 0.5 cm step and a constant integration time of 2 s. The baseline was acquired with the corresponding buffer, under strictly the same conditions and then subtracted from the spectrum of the sample. A similar procedure was used for near-UV CD spectra, between 250 and 350 nm, except that the path length was 1 cm instead of 0.02 cm. During acquisition, the temperature of the cell holder was controlled by circulating water at constant temperature from a water bath.

RESULTS

Urea-Induced Fibronectin Denaturation. Fibronectin contains a large number of tryptophan residues (around 80) essentially localized inside the different globular modules of the molecule and disposed in a homogeneous way along the chain. On the basis of this feature, steady-state fluorescence emission intensity and emission maxima of tryptophan residues were used as probes of the urea-induced denaturation of the protein under different ionic strength conditions.

As shown in Figure 1, in absence of denaturant, fibronectin has a maximum fluorescence emission centered at 330 nm, indicating that the majority of the tryptophans are buried in the folded protein. The same result is observed at low and high ionic strength (1 mM Tris-HCl, pH 7.4, and 10 mM Tris-HCl + 150 mM NaCl, pH 7.4; panels A and B of Figure 1, respectively). These data indicate that, at 0 M urea, ionic strength, in the range tested, has no effect on the tertiary structure of fibronectin. Consequently, we called this state "native state".

In 10 M urea, the fluorescence emission maximum is red shifted to 350 nm, indicating that urea at high concentration

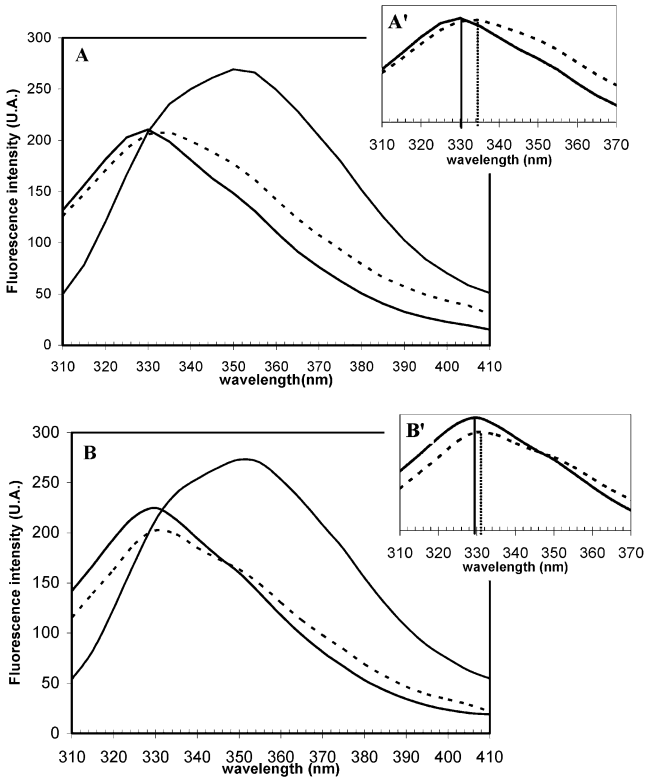

FIGURE 1: Fluorescence emission spectra of fibronectin during the denaturation process. The samples were excited at 295 nm. In both panels, fibronectin (0.1 μM) was incubated for 24 h at 24 °C in 1 mM Tris-HCl, pH 7.4 (panel A), containing urea at 0 M (solid line), 4 M (dotted line), and 10 M (gray line), or in 10 mM Tris-HCl and 150 mM NaCl, pH 7.4 (panel B), containing urea at 0 M (solid line), 4 M (dotted line), and 10 M (gray line). Panels A′ and B′ show the λ_{max} emission of fibronectin in 1 mM Tris-HCl, pH 7.4, and 10 mM Tris-HCl and 150 mM NaCl, pH 7.4, respectively.

induces an unfolding of the protein, with exposure of its tryptophan residues to solvent. However, the fluorescence spectrum presents a shoulder around 330 nm, which indicates the persistence of some nativelike structures. Nevertheless, the urea-induced fluorescence dramatic change reveals a marked alteration of the tertiary structure. In addition, the far-UV CD spectrum (data not shown) of the urea-treated fibronectin showed a large ellipticity change, indicating the loss of secondary structure. This state of fibronectin is thus called "unfolded state" in the following.

At intermediate urea concentrations (around 4 M), some differences, depending on ionic strength conditions, appear in emission spectra. Representative data are shown in Figure 1, panels A′ and B′, for protein in 4 M urea (dotted line). On one hand, at high ionic strength, the emission maximum at 4 M urea is centered around 331 nm, close to the value obtained for fibronectin at 0 M urea (Figure 1, panels B and B′). This indicates that the tertiary structure of fibronectin is only slightly affected by urea at 4 M. On the other hand, at low ionic strength and the same urea concentration (4 M), the fluorescence emission spectrum was clearly red shifted compared to that of the native protein: its maximum is 335 nm instead of 330 nm in the absence of urea (Figure 1, panels A and A′). This red shift was observed at any concentration ranging from 3 to 4 M urea under low ionic strength conditions (data not shown). This observation suggests the accumulation of an equilibrium unfolding intermediate

between 3 and 4 M urea, under these conditions of ionic strength.

Thus, it seems that the unfolding process of fibronectin could be different according at low and high ionic strength, with or without accumulation of a partially folded state.

Effect of Ionic Strength on the Equilibrium Unfolding of Fibronectin. (A) Fluorescence Measurement. Urea-induced denaturation of fibronectin has been studied at five different ionic strengths: two referred to as low, water 18 MΩ and 1 mM Tris-HCl, pH 7.4, and three referred to as high, 10 mM Tris-HCl, pH 7.4, 10 mM Tris-HCl + 30 mM NaCl, pH 7.4, and 10 mM Tris-HCl + 150 mM NaCl, pH 7.4 (see Materials and Methods).

Figure 2 shows the influence of the ionic strength on the urea-induced transition of fibronectin by investigating the environment of the tryptophan residues as followed by emission intensity at 360 nm. As can be seen in Figure 2A,B (open circle), under the two low ionic strength conditions, there is almost no change between 0 and 1.8 M urea. A first cooperative increase of the signal was observed between 2 and 3 M urea. Then a second cooperative transition occurred between 5 and 7 M urea. These data showed that, under these low ionic strength conditions, the complete unfolding of fibronectin seems to obey a three-state unfolding process, with a well-populated folding intermediate accumulating at 3−4 M urea. On the contrary, the unfolding transitions of fibronectin at high ionic strength, as shown in Figure 2C−E (open circle), reveal a single cooperative transition that occurs between 4 and 8 M urea.

So, it appears that ionic strength induces an important difference in the denaturation pathway of fibronectin.

To characterize more precisely the unfolding at the different ionic strengths tested, we analyzed the transition curves using a nonlinear least-squares fit of the different set of data.

Since the transition profiles collected under the low ionic strength condition (Figure 2A,B) obviously revealed the transient accumulation of a stable intermediate around 3−4 M urea, the experimental data have been first fitted according to a three-state model. After convergence, a nonrandom deviation between the simulated curve and the experimental data was systematically observed, whatever the fitting procedure used. Therefore, we concluded that the equilibrium denaturation process of fibronectin did not obey a three-state transition. This result suggested that a more complicated unfolding mechanism, implying at least three steps and two intermediate states should occur under weak ionic strength conditions.

According to the same approach as above, we fitted the data collected at high ionic strength to the minimum two-state transition. In this case, again the fit was clearly not satisfactory since the curve calculated from the best fit showed a marked deviation from the experimental data. The sequential three-state model did not satisfactorily account either for our experimental data and still led to an important statistical error (data not shown). Thus, again in this case, the fitting analysis clearly indicates that a minimum three-stage model had to be considered.

The five series data (at either ionic strength) were then fit to the sequential four-state model with much better results, as shown in Figure 2 (solid lines). In this case, whatever the ionic strength was, the good correlation between the experimental data and the simulated curves obtained from the best fits indicates that this equilibrium-unfolding model was suitable.

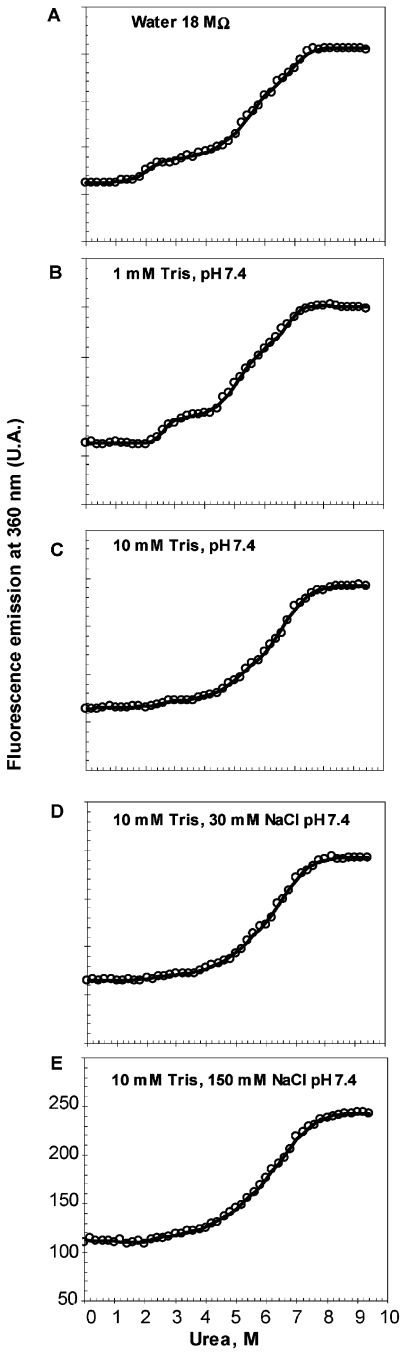

FIGURE 2: Equilibrium denaturation of fibronectin. Denaturation was measured by fluorescence emission at 360 nm with excitation at 295 nm. In all experiments, the protein concentration was 0.1 μM. Each sample was measured after 24 h incubation. The data were fit simultaneously (solid lines) as described under Materials and Methods using the development of eq 26.

On the basis of this minimum three-stage equilibrium model, we determined the conformational free energy, ΔG^{H_2O}, and the *m* values (see Materials and Methods) for each step during the denaturation process. Table 1 summarizes the values of the thermodynamic parameters deduced from the best fits under the different ionic strength conditions. In water, 18 MΩ, the free energy changes $\Delta G°_1$ (N ⇔ I_1), $\Delta G°_2$ (I_1 ⇔ I_2), and $\Delta G°_3$ (I_2 ⇔ U) were respectively 10.5 ± 0.4, 8.6 ± 0.3, and 15.0 ± 0.4 kcal/mol. Thus the global

Table 1: Thermodynamic Parameters Characterizing the Denaturation Process of Fibronectin[a]

	fluorescence						
ionic strength conditions	$\Delta G°_1$[b]	m_1[c]	$\Delta G°_2$[b]	m_2[c]	$\Delta G°_3$[b]	m_3[c]	$\Delta G°_t$[b]
water, 18 MΩ	10.5 ± 0.4	4.8 ± 0.5	8.6 ± 0.3	1.8 ± 0.2	15.0 ± 0.4	1.8 ± 0.3	34.2 ± 0.6
1 mM Tris-HCl, pH 7.4	9.9 ± 0.2	3.6 ± 0.2	6.6 ± 0.3	1.2 ± 0.15	13.7 ± 0.8	1.8 ± 0.4	30.2 ± 0.8
10 mM Tris-HCl, pH 7.4	10.6 ± 0.4	4.4 ± 0.3	4.5 ± 0.3	1.0 ± 0.1	7.4 ± 0.3	1.2 ± 0.2	22.5 ± 0.7
10 mM Tris-HCl, 30 mM NaCl, pH 7.4	10.8 ± 0.4	5.0 ± 0.2	4.2 ± 0.2	1.0 ± 0.1	7.4 ± 0.1	1.1 ± 0.1	22.5 ± 0.5
10 mM Tris-HCl, 150 mM NaCl, pH 7.4	10.7 ± 0.4	5.1 ± 1.2	4.2 ± 0.3	1.0 ± 0.1	7.3 ± 0.1	1.1 ± 0.1	22.2 ± 0.4

[a] The denaturation transitions under various ionic strength conditions were fitted to eq 26 as developed in Materials and Methods. For each parameter, the values correspond to the average of values calculated by nonlinear square fitting from the three independent sets of data. The errors correspond to the standard deviation calculated from average values of the corresponding parameter. [b] In kcal·mol^{-1}. [c] In kcal·mol^{-1}·M^{-1}.

free energy change $\Delta G°_t$ associated with the N ⇔ U transition in water, 18 MΩ, obtained by summing the free energy changes of the individual steps, is 34.2 ± 0.6 kcal/mol. Similarly, the global free energy change was calculated for the unfolding transition at other ionic strengths. The corresponding values of $\Delta G°_t$ for the N ⇔ U equilibrium in 1 mM Tris-HCl, pH 7.4, 10 mM Tris-HCl, pH 7.4, 10 mM Tris-HCl + 30 mM NaCl, pH 7.4, and 10 mM Tris-HCl + 150 mM NaCl, pH 7.4, are 30.2 ± 0.8, 22.5 ± 0.7, 22.5 ± 0.5, and 22.2 ± 0.4 kcal/mol, respectively. So, the global free energy change decreases with increasing the ionic strength.

When comparing the free energy change of each individual step, we observed no significant change with the ionic strength for the N ⇔ I_1 transition conditions (average value: 10.5 kcal/mol). Concerning the second step, I_1 ⇔ I_2, the calculated values of $\Delta G°_2$ decrease with increasing the ionic strength. Similarly, the free energy change of the third transition, I_2 ⇔ U, decreases when ionic strength increases. Thus, the decrease of the global free energy change with increasing ionic strength is related to both transitions I_1 ⇔ I_2 and I_2 ⇔ U, the conversion of N to I_1 being insensitive.

To evaluate the transient accumulation of the different species along the urea-induced unfolding, the equilibrium distribution of the four species, N, I_1, I_2, and U, as a function of urea concentration could be reconstituted using the fitted values of $\Delta G°_1$, $\Delta G°_2$, $\Delta G°_3$, m_1, m_2, and m_3 (see Table 1). Similar curves are obtained for the two low and the three high ionic strength conditions. As examples, Figure 3 shows these distribution curves for 1 mM Tris-HCl, pH 7.4, and 10 mM Tris-HCl + 150 mM NaCl, pH 7.4. As can be seen, the main difference between the two situations is the lower accumulation of the second intermediate I_2 at high ionic strength compared to that at low ionic strength.

(B) Fluorescence Quenching. As previously established, the equilibrium unfolding processes of fibronectin, at any ionic strength tested, can be well described by the sequential four-state equilibrium model. On the basis of this model, ionic strength affects the thermodynamic parameters ($\Delta G°$ and m) associated with the two last steps, changing the extent of accumulation of the intermediates. In the analysis of the steady-state tryptophan fluorescence spectra and particularly emission maxima, some differences between low and high ionic strength conditions were evidenced, especially at intermediate denaturant concentration, between 3.4 and 4 M urea, where the first intermediate state (I_1) accumulates. As previously mentioned, the accumulation of I_1 is only slightly more pronounced under low ionic strength condition. This suggests that I_1 is not corresponding to the same species at high and at low ionic strength. The structural distinction

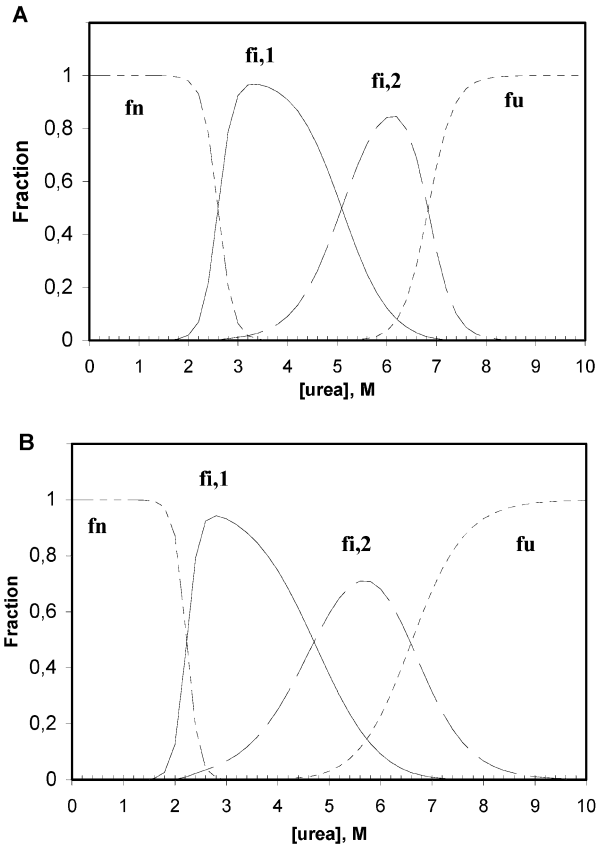

FIGURE 3: Distribution of the native, intermediate, and unfolded state of fibronectin as a function of urea concentration. The fractions of native (f_n), the first intermediate (f_{i1}), the second intermediate (f_{i2}), and the unfolded (f_u) states were calculated using the parameters deduced from the fits of the denaturation transitions in (A) 1 mM Tris, pH 7.4, and (B) 10 mM Tris-HCl and 150 mM NaCl, pH 7.4.

between I_1 in both conditions might reflect a difference in conformational flexibility. Fibronectin contains a large amount of tryptophan residues, and each of them is characterized by its microenvironmental properties. Depending on their localization in the protein, these tryptophans are accessible to the solvent to various extents, according to the conformational flexibility and the extent of individual accessibility of a particular residue varied along the denaturation transition. Fluorescence quenching experiments have been proved to give precise information about local conformational fluctuation around tryptophans. We thus used this approach to compare the conformational flexibility of the intermediate state I_1 at low and high ionic strength. Quenching experiments were realized with fibronectin in the absence or in the presence of urea at 3.4, 4, and 10 M urea, under

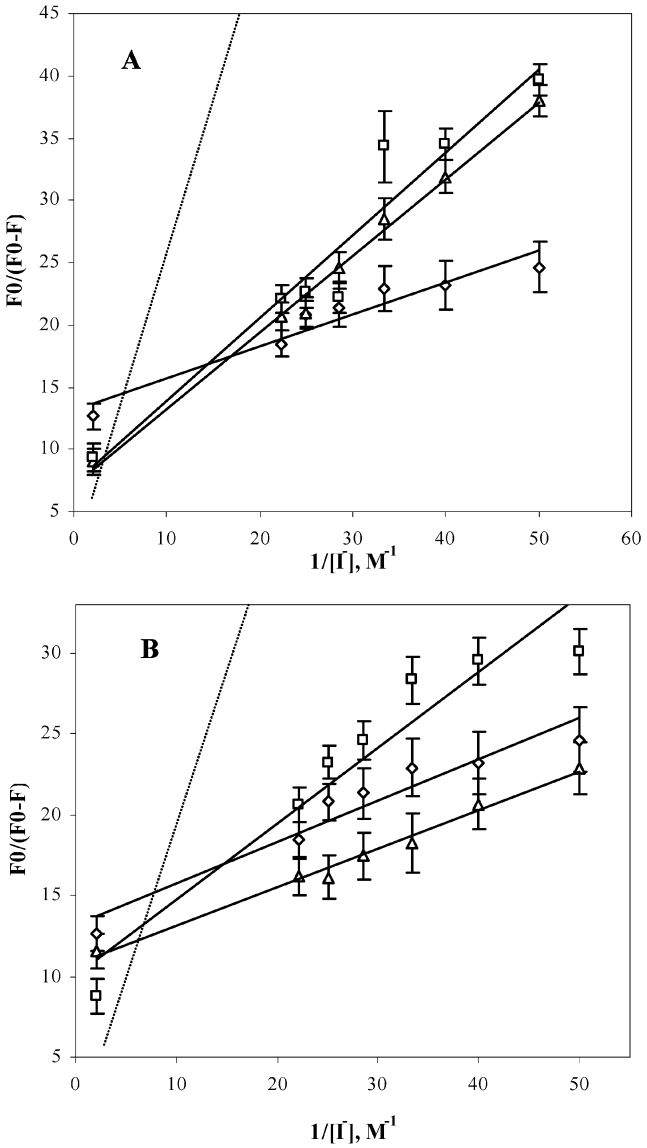

FIGURE 4: Lehrer plot of the tryptophan fluorescence quenching of fibronectin by iodide. Quenching of fluorescence was measured on fibronectin under its native state (triangle) and intermediate state at 3.4 M urea (rhombus) and 4 M urea (square) in 1 mM Tris-HCl, pH 7.4 (panel A), or in 10 mM Tris-HCl and 150 mM NaCl, pH 7.4 (panel B). In both panels, the solid lines correspond to the linear regression of the data sets, and the dotted line corresponds to the quenching of free tryptophan in solution in the related buffer.

low (10 mM Tris-HCl, pH 7.4) and high (1 mM Tris-HCl, 150 mM NaCl, pH 7.4) ionic strength conditions. The selective ion I^- was used as a quencher to preferentially probe tryptophans near the surface of the protein. A solution-free tryptophan in the presence of gelatin (which mimics protein environment) was also used as a standard to evaluate the complete accessibility to quencher. The results were analyzed according to the Lehrer representation by plotting $F_0/(F_0 - F)$ as a function of $1/[I^-]$, F_0 and F being the fluorescence intensity in the absence and at a given quencher concentration $[I^-]$. The results are shown in Figure 4, but concerning fibronectin unfolding states, the curves were omitted for clarity. Values of the accessible fraction, $(f_a)_{eff}$, for the different states were obtained from the intercept of the curves, and K_{eff} (i.e., constant of Stern−Volmer when protein contains only one population of tryptophan residues) was deduced from the slope of the linear part of the curves. These values are listed in Table 2.

Table 2: Fluorescence Quenching of Fibronectin and Free Tryptophan by Iodide[a]

	1 mM Tris-HCl, pH 7.4		10 mM Tris-HCl, 150 mM NaCl, pH 7.4	
	K_{eff} (M^{-1})	f_a (%)	K_{eff} (M^{-1})	f_a (%)
native state (0 M urea)	0.26 ± 0.07	8 ± 2	0.26 ± 0.07	8 ± 2
intermediate state (3.4 M urea)	0.61 ± 0.14	14 ± 2	0.23 ± 0.11	9 ± 2
intermediate state (4 M urea)	0.66 ± 0.15	14 ± 1	0.47 ± 0.16	11 ± 2
unfolding state (10 M urea)	2.69 ± 0.12	73 ± 3	2.25 ± 0.10	68 ± 3
free tryptophan	3.31 ± 0.11	85 ± 3	3.25 ± 0.09	87 ± 3

[a] K_{eff} represents the Stern−Volmer constant for proteins containing several populations of tryptophan residues and f_a the accessible fraction of tryptophan quenched by iodide.

The values of K_{eff} (0.26 M^{-1}) and $(f_a)_{eff}$ (8%) for the native state (i.e., in absence of urea) are unaffected by the ionic strength. At intermediate urea concentration (3.4 and 4 M) some differences appear between low and the high ionic strength conditions. In 1 mM Tris-HCl, pH 7.4 (Figure 4A), similar Lehrer plots were observed at 3.4 and 4 M urea, with values of K_{eff} and $(f_a)_{eff}$ of over 0.6 M^{-1} and 14%, respectively. In contrast, K_{eff} and $(f_a)_{eff}$ at high ionic strength (10 mM Tris-HCl, 150 mM NaCl, pH 7.4; see Figure 4B) are substantially lower and in addition differ between 3.4 and 4 M urea (0.23 M^{-1} and 9% vs 0.47 M^{-1} and 11%; see Table 2). This last difference probably comes from the overlapping between the distribution curves in the range 3.4−4 M urea, more pronounced at high than at low ionic strength. As shown in Figure 3, at low ionic strength, the contamination of I_1 by I_2 in 3.4 M urea is roughly the same as that at 4 M urea at high ionic strength. On the other hand, the difference in K_{eff} and $(f_a)_{eff}$ at 3.4 M urea between low and high ionic strength clearly reveals that the first folding intermediate I_1 is more flexible at low ionic strength.

(C) Far- and Near-UV Circular Dichroism Analysis. Far- and near-UV CD has been used to study the effect of ionic strength on the secondary and tertiary structures of fibronectin in different unfolded states. Figure 5A shows the far-UV CD spectra of fibronectin at 0, 4, and 10 M urea under low and high ionic strength conditions (1 mM Tris-HCl, pH 7.4, and 10 mM Tris-HCl, 150 mM NaCl, pH 7.4). First, we can observe that, despite a difference in amplitude between the native state spectra recorded under the two ionic strength conditions, the general shape is the same. Moreover, the ratio of the CD amplitude at all wavelengths is constant. Thus this difference is probably due to the concentration accuracy. Indeed, we used the same value of the extinction coefficient at 280 nm, in both conditions, whereas this parameter may be affected by the salt concentration. We thus considered that the secondary structure in the native state was insensitive to the ionic strength. The large negative CD amplitude centered at 212 nm indicates that native fibronectin has a secondary structure essentially organized around β-sheets.

In 10 M urea, the protein clearly lost its β-sheet structures. However, the positive amplitude between 220 and 240 nm remains. Because the unfolding occurred without any reduc-

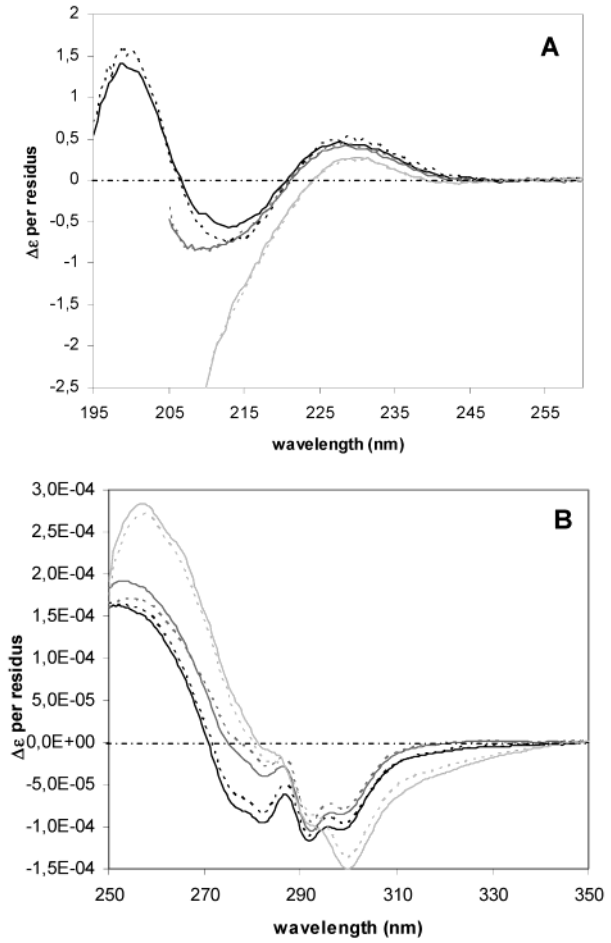

FIGURE 5: Circular dichroism of fibronectin under various states along its denaturation process. Far-UV (panel A) and near-UV (panel B) CD spectra were recorded with fibronectin in 1 mM Tris-HCl, pH 7.4 (solid lines), or in 10 mM Tris-HCl and 150 mM NaCl, pH 7.4 (dotted lines), at 0 M urea (black lines), 4 M urea (gray line), and 10 M urea (light gray lines). In all cases, the protein concentration was 2 μM.

ing agent, this CD band likely corresponds to the contribution of disulfide bonds to the far-UV CD.

At 4 M urea, the concentration corresponding to the accumulation of the first intermediate I_1, the far-UV CD spectra recorded at low and high ionic strength superimposed. The slight blue shift of the negative band between 205 and 222 nm accompanied by the slight decrease of the minimum indicates a partial conversion of β-sheets to unordered structures. Thus, at 4 M urea, the intermediate state has the same secondary structure content at low and high ionic strength, and its secondary structure content is closer to that of the native protein rather than to the unfolded one.

Figure 4B shows the near-UV CD spectra of fibronectin in 0, 4, and 10 M urea recorded between 250 and 350 nm at low and high ionic strength under the same conditions described above for the far-UV CD data. These near-UV CD spectra reflect the environments of the aromatic amino acid side chains and thus give information about the tertiary structure of the fibronectin. We observed, under a particular ionic strength condition, a decrease in the negative peak intensity at 283 nm when urea concentration was increased. These results confirm that urea affects the tertiary as well as the secondary structure organization of fibronectin. Comparing high and low salt concentrations, we noted that at either urea concentration tested the CD intensity in the tryptophan resonance region is systematically lower at high ionic condition. This effect indicates an effect of ionic strength on the tertiary structure organization in the different urea-induced states of fibronectin.

DISCUSSION

Combination of fluorescence and circular dichroism spectroscopy allowed us to investigate the secondary and tertiary structure evolution and to determine the thermodynamics parameters of stability along the denaturation process induced by urea under different ionic strength conditions. We have described conditions for equilibrium unfolding of fibronectin in urea-containing buffer with various ionic strength, monitored by intrinsic fluorescence. There is an evident red shift in the fluorescence emission spectrum when the protein is incubated in urea at intermediate concentration (around 4 M) at low ionic strength. This suggests that under these conditions the tryptophan residues are partially exposed to solvent. Moreover, this red shift is observed between 3 and 4 M urea, suggesting the existence of an unfolding intermediate state. This shift is less marked in the same urea concentration range at higher ionic strength. Under strong denaturant conditions, at 10 M urea, whatever the ionic strength, both the increase in intensity at 350 nm and the red shift in the fluorescence emission spectrum indicate an unfolding of the protein.

Some precautions have been taken to ensure that the observed effect could not be due to experimental artifacts such as pH variations or aggregation process. Indeed, for the experiments at low ionic strength, pure water and 1 mM Tris-HCl, pH 7.4, have been used, and in such no or weakly buffered solutions, some pH variation could appear. So, we checked that the difference in the fibronectin denaturation pathway is exclusively due to ionic strength and not to pH variation. For this purpose, the pH of each sample was controlled before and after measurements, and we observed that, despite the weak ionic strength used, the pH variations were negligible. This control clearly confirms that the difference in denaturation pathway of fibronectin including the accumulation of an intermediate state in urea concentration above 3−4 M urea is exclusively dependent on ionic strength.

Moreover, at high ionic strength, the value of κ^{-1} indicates that intra- and intermolecular electrostatic interactions are not negligible and could induce aggregation of fibronectin. So, we analyzed precisely fibronectin absorption spectra at different urea concentrations (0, 3.4, 4, and 10 M) under the different ionic strength conditions tested (data not shown). No turbidity was detected above 320 nm, where there is no expected absorption of the protein, indicating that no aggregation of fibronectin occurred in urea-containing solutions.

Ionic Strength Contribution on Fibronectin Denaturation Pathway. To characterize precisely the ionic strength-induced difference in the denaturation pathway of fibronectin, the fluorescence dependence toward urea concentration has been fitted to several models, and in all cases, the data are well described by at minimum four-state equilibrium. Such an unfolding process has been previously reported in the case of procaspase-3, a homodimeric protein (*24*). To correlate

unfolding of this protein to a biological meaning, we investigated more precisely the $\Delta G°$ value associated with each step along the transition.

Concerning the first step, whatever ionic strength used, around 10.0 kcal/mol is needed to convert the native state N to the first intermediate I_1. The $\Delta G°_2$ corresponding to the second transition, i.e., $I_1 \leftrightarrow I_2$, appears to vary with the ionic strength; it drops from 8.6 ± 0.3 to 4.2 ± 0.3 kcal/mol from the lowest to the highest ionic strength tested. The free energy change of the third step, $I_2 \leftrightarrow U$, also decreases from 15.0 ± 0.4 to 7.3 ± 0.1 kcal/mol when the ionic strength increases.

In a previous work, Litvinovitch et al. (*25*) reported that the free energy change necessary to unfold the type III domain of fibronectin is 10 kcal/mol. However, 2 years later Erickson (*26*) demonstrated that, taking into account energetic considerations, an additional 5 kcal/mol is needed to obtain the complete unfolding of this isolated domain. More recent studies reported that stretching of native fibronectin begins by type III modules unfolding (*27*). Indeed, the increase in contour length is around 28.5 nm, a distance that is consistent with the length of an unfolded FNIII domain. Furthermore, the results obtained by stretching experiments (*28*) can be compared with our results from chemical denaturation, since a possible correlation between mechanical and traditional unfolding has been clearly demonstrated.

Thus, we can reasonably postulate that the first step in the urea-induced denaturation of the entire fibronectin would correspond to the partial unfolding of type III modules, while the second steps, leading to the second intermediate, would result in the complete unfolding of these type III modules. Thus, the two first steps ($N \leftrightarrow I_1$ and $I_1 \leftrightarrow I_2$) could be attributed to a hierarchical denaturation of the type III modules. This result, observed for the first time on the whole fibronectin, is consistent with the previous data of Oberhauser et al. on FNIII modules (*26*), who postulate such a mechanism using atomic force microscopy.

According to this hypothesis, the last step which leads to the totally unfolded state would imply both the 12 FNI and the 2 FNII modules. These modules are shorter than FNIII, with 45 and 60 residues, respectively, and contain internal disulfide bonds that are likely to prevent their denaturation.

Ionic Strength Effect on Fibronectin Stability. Conformational free energies and *m* values for each step in the equilibrium unfolding have been calculated. The data clearly indicate a difference in protein stability under low or high ionic strength conditions. Indeed, the difference in conformational free energy for the global $N \leftrightarrow U$ transition, between low and high ionic strength conditions, is 12.0 ± 0.7 kcal/mol (34.2 ± 0.6 versus 22.2 ± 0.4 kcal/mol, respectively). So, fibronectin appears clearly more stable in low ionic strength conditions.

We also calculated the midpoint urea concentration for the three steps of the transition (depending on the respective $\Delta G°$ and *m* values). The midpoint urea concentration of the first step was found to be 2.5 M urea and independent of the ionic strength. This result confirms that the first transition step is definitely not affected by the ionic strength. On the contrary, as expected, the midpoint values for the second and the third step transitions vary with ionic strength. When the ionic strength increases, the midpoints of the second and third transition are shifted to lower urea concentration. These changes corroborate the decrease in the corresponding $\Delta G°$ values.

To explain this ionic strength effect, it is necessary to consider the electrostatic interaction contributions that could exist in fibronectin. Indeed, it is generally accepted that electrostatic interactions on protein surface, such as ion pairs, could contribute to protein stability and could play an important role in the conformational specificity (*29*, *30*). Analysis of the free energy change associated with the $N \leftrightarrow I_1$ transition indicates that this step is not affected by the ionic strength conditions used. One hypothesis is that one part of the FNIII domain (the part implied in this transition) is slightly stabilized by electrostatic forces but preferably maintained by other contributions such as hydrophobic interactions, van der Waals forces, and hydrogen bonds (*31*, *32*). On the contrary, the free change energy associated with the $I_1 \leftrightarrow I_2$ step, which permits the complete unfolding of the FNIII domain, is affected by the ionic strength conditions. So, we can now suppose that this last part of the FNIII domain is mainly stabilized by electrostatic interactions. For example, it has been experimentally shown that when attractive electrostatic interactions are attenuated, the stability of $FNIII_{10}$ decreases (*33*). Thus, the conformational stability of the $FNIII_{10}$ module can be enhanced by adjusting electrostatic properties, so that an increase in ionic strength results in removing the unfavorable electrostatic interactions on protein surface.

Concerning the last transition step, $I_2 \leftrightarrow U$, the influence of ionic strength is more obvious. To understand this important effect, we analyzed charge repartition inside the modules implicated in this third transition. In the type I module, the most represented module, about one-third among the 45 residues on average are charged. Also, the charge mean distribution is balanced. So, electrostatic attractive interactions could largely contribute to the stability of this type of module. An increase in ionic strength could lead to a screening charge effect. Attenuation of these attractive electrostatic interactions could then destabilize the modules. This effect is concomitant with an increase of ionic strength in the range used. Consequently, a shift to a lower concentration of urea as well as a decrease of $\Delta G°_3$ should be observed. These results confirmed this prediction. First, the species distribution clearly indicates that high ionic strength attenuates accumulation of the intermediate state and promotes, from an energetic point of view, the different transitions. Second, the quenching fluorescence measurements evidence a stable intermediate state between 3.4 and 4 M urea under low ionic strength conditions, whereas under the same conditions, at high ionic strength conditions, the detected intermediate appears to be less accumulated. These data confirm that an increased ionic strength destabilizes this intermediate state. Such effect of ionic strength contribution to the stabilization of an intermediate state has been previously observed for other multidomain proteins such as human serum albumin (*34*). This study reports that an increase of anions in solution during a urea-induced denaturation process prevents the formation of the intermediate state, and the authors suggest that the electrostatic binding of anions to the positively charged sites of human serum albumin is the major factor responsible for the anion-induced conformational stabilization.

Concerning the denaturation extent of fibronectin at high urea concentration, it must be noted that in 10 M urea, whatever the ionic strength conditions used, the conformation could be grossly considered as a "random coil", though, due to the preservation of the disulfide bridges, restricted regions probably retain some residual structure. Indeed, from the apparent difference in the K_{eff} value of fibronectin in 10 M urea compared to that of free tryptophan, the protein cannot strictly be considered as completely unfolded. We thus came to the conclusion that fibronectin should be considered as a chain of small globular domains behaving like an individual protein, for it has been shown that denaturant concentrations as high as 8 M urea do not always induce a complete unfolding of small globular proteins (*35*). Persistence of disulfide bonds obviously reinforces this resistance to complete unfolding. As a matter of fact, when denatured at 10 M urea in the presence of dithiothreitol, the fluorescence emission spectrum showed an enhanced red shift (355 instead of 350 nm in the absence of reducing agent) and an increase in fluorescence intensity (data not shown). A disruption of the intermolecular and intramolecular disulfide bonds thus leads to the complete fibronectin unfolding. However, in previous works, from scattering experiments, a completely unfolded state of fibronectin has been supposed to occur in 8 M urea (*9*). These results, in apparent contradiction, have to be attributed to differences between structural and conformational point of views.

In summary, here we demonstrate that the denaturation process implies intermediate states with stability affected by ionic strength conditions. At low ionic strength, the first intermediate accumulated is more stable than the intermediate state detected at high ionic strength. Due to this observation, one hypothesis is that the ionic strength effect participates in the structuring of the intermediate states.

Ionic Strength Effect on Fibronectin Structure. The folded conformation can be disrupted by environmental changes not involving variations in covalent structure (*26*). Near-UV CD data reveal, at high ionic strength, minor changes in the tertiary structure of fibronectin in its native state. However, the secondary structure of the native state is not affected by the ionic strength conditions, as shown by comparison of the related far-UV CD spectra. These results suggest that increasing the ionic strength could imply variations in the topology of loops and turns, changing the force pattern that stabilizes the β-strands and the tertiary structure of the protein. These changes do not affect the secondary structure distribution but decrease the urea concentration necessary to unfold the protein by weakening the interactions between strands. This situation has been shown in the case of lentil lectin, an all-β-sheet protein. In this case, pH in the range of 5.0−10.0 induces no significant change in the overall secondary structure observed but affects β-sheet and β-turn cross-interactions in a way that makes the protein more sensitive to the heat-induced denaturation (*36*).

Biological Implication of the Fibronectin Intermediate State. During development, wound healing, and other processes involving extracellular matrix remodeling, fibroblasts secrete soluble FN and assemble it into insoluble fibrils. The process involves FN binding to the cell, mechanical coupling of FN to the cytoskeleton by integrins, exposure of self-assembly sites via contractile cell forces, and elongation of fibrils by FN polymerization (*37*, *38*). The initial cell attachment, exposure of the integrin binding arginine−glycine−aspartic acid (RGD) loop, and availability of self-assembly sites are likely regulated by fibronectin conformation. Indeed, steered molecular dynamics simulations predict that, before unraveling of FNIII modules, the buried cryptic sites between adjacent modules could be exposed in the intermediate state obtained from the force application leading to the partially unfolding state of FNIII modules (*39*). Stretching FNIII modules into this intermediate state requires less force than breaking apart the first β-strands. Moreover, steered molecular dynamics simulations predict that stretching the $FNIII_{10}$ module into this intermediate state reduces $\alpha_5\beta_1$ integrin binding (*16*). Besides, a recent work indicates that perturbing the native conformation of the $FNIII_9$ synergy site, required for efficient integrin $\alpha_5\beta_1$ binding and cell adhesion, leads to impaired domain stability (*40*). Indeed, a mutation into the RGD−PHSRN−synergistic sequence of $FNIII_{9-10}$ not only has a negative effect on the adhesion of baby hamster kidney fibroblasts (which leads to a reduced ability of these ligands to recognize integrin $\alpha_5\beta_1$) but also has a strong negative effect on the thermodynamic stability of the $FNIII_9$ domain.

In conclusion, it could be admitted that conformation and stability of different fibronectin states play a crucial role in the regulation of fibronectin interaction with other molecules, such as integrin, or other fibronectin molecules during the fibrillogenesis process (*41*, *42*). Our results demonstrate for the first time that this hierarchical FNIII module unfolding (implicated in biological processes and largely illustrated on the isolated module by theoretical and experimental approaches) is applied to the whole fibronectin. Moreover, whatever the ionic strength conditions used, the fibronectin unfolding pathway implicates a (minimum) four-state mechanism with, in particular, a sequential two-stage unfolding of the FNIII module. Nevertheless, despite this analogy in unfolding pathways, some differences exist concerning both the energetic contribution needed for the transition and the structure organization of the intermediate states. Indeed, it clearly appears that subtle structural reorganizations exist in fibronectin due to the ionic strength effect, i.e., electrostatic contribution that could contribute in vivo to the modulation of fibronectin behavior. Hence, conformational stability and hierarchical unfolding could significantly modulate the binding properties of fibronectin to cell and matrix molecules.

ACKNOWLEDGMENT

We acknowledge the Laboratoire du Fractionnement and des Biotechnologies des Ulysses (France) for a generous gift of human plasma cryoprecipitate. We thank Dr. Yves Gaudin for advice concerning fluorescence spectroscopy and Dr. Juan Pelta for fruitful discussions about the effects of ionic strength on fibronectin conformation and for contribution to the work. We are grateful to Stephane Lioret (Hull University, U.K.) for kindly correcting the language of the manuscript.

REFERENCES

1. Ruoslahti, E. (1988) *Annu. Rev. Biochem. 57*, 375−413.
2. Hynes, R. O. (1990) *Fibronectins*, Springer, New York.
3. Hynes, R. O. (1999) *Proc. Natl. Acad. Sci. U.S.A. 96*, 2588−2590.
4. Potts, J. R., and Campbell, I. D. (1994) *Curr. Opin. Cell Biol 6*, 648−655.

5. Tsyguelnaia, I., and Doolittle, R. F. (1998) *J. Mol. Evol. 46*, 612−614.
6. Yamada, K. M. (1989) in *Fibronectin* (Mosher, D. F., Ed.) pp 48−12, Academic Press, New York.
7. Dickinson, C. D., Veerapandian, B., Dai, X.- P., Hamlin, R. C., Xuong, N.-H., Ruoslahti, E., and Ely, K. R. (1994) *J. Mol. Biol. 236*, 1079−1092.
8. Williams, M. J., Phan, I., Harvey, T. S., Rostagno, A., Gold, L. I., and Campbell, I. D. (1994) *J. Mol. Biol. 235*, 1302−1311.
9. Pelta, J., Berry, H., Fadda, G. C., Pauthe, E., and Lairez, D. (2000) *Biochemistry 39*, 5146−5154.
10. Koteliansky, V. E., Glukova, M. A., Bejanian, M. V., Smirnov, V. N., Filimonov, V. V., Zalite, O. M., and Venyaminov, S. Yu. (1981) *Eur. J. Biochem. 119*, 619−624.
11. Pauthe, E., Pelta, J., Patel, S., Lairez, D., and Goubard, F. (2002) *Biochim. Biophys. Acta 1597*, 12−21.
12. Zhong, C., Chrzanowska-Wodnicka, M., and Brown, J. (1998) *J. Cell Biol. 141*, 539−551.
13. Ingham, K. C., Brew, S. A., Huff, S., and Litvinovich, S. V. (1997) *J. Biol. Chem. 272*, 1718−1724.
14. Sechler, J. L., Rao, H., Cumiskey, A. M., Vega-Colon, I., Smith, M. S., Murata, T., and Scharzbauer, J. E. (2001) *J. Cell Biol. 154*, 1081−1088.
15. Litvinovich, S. V., Brew, S. A., Aota, S., Akiyama, S. K., Haudenschild, C., and Ingham, K. C. (1998) *J. Mol. Biol. 280*, 245−258.
16. Krammer, A., Craig, D., Thomas, W. E., Schulten, K., and Vogel, V. (2002) *Matrix Biol. 21*, 139−147.
17. Benecky, M. J., Wine, R. W., Kolvenbach, C. G., and Mosesson, M. W. (1991) *Biochemistry 30*, 4298−430.
18. Poulouin, L., Gallet, O., Rouahi, M., and Imhoff, J. M. (1999) *Protein Expression Purif. 17*, 146−142.
19. Dobrynin, A. V., Rubinstein, M., and Colby, R. (1995) *Macromolecules 28*, 1859−1871.
20. Stern, O., and Volmer, M. (1919) *Phys. Z. 20*, 183−193.
21. Lehrer, S. S. (1971) *Biochemistry 80*, 3254−3263.
22. Pace, C. N. (1986) *Methods Enzymol. 131*, 266−280.
23. Thompson, J., Shirley, B., Grimsley, G., and Pace, C. (1989) *J. Biol. Chem. 264*, 11614−11620.
24. Bose, K., and Clark, A. C. (2001) *Biochemistry 40*, 14236−142342.
25. Litvinovich, S. V., Novokhatny, V. V., Brew, S. A., and Ingham, K. C. (1992) *Biochim. Biophys. Acta 1119*, 57−62.
26. Erickson, H. P. (1994) *Proc. Natl. Acad. Sci. U.S.A. 91*, 10114−10118.
27. Oberhauser, A. F., Badilla-Fernandez, C., Carion-Vazquez, M., and Fernandez, J. M. (2002) *J. Mol. Biol. 319*, 433−447.
28. Carrion-Vazquez, M., Oberhauser, A. F., Fowler, S. B., Marszalek, P. E., Broedel, S. E., Clarke, J., and Fernandez, J. M. (1999) *Proc. Natl. Acad. Sci. U.S.A. 96*, 3694−3699.
29. Creighton, T. E. (1993) *Proteins: Structures and molecular properties*, Freeman, New York.
30. Dao-Pin, S., Sauer, U., Nicholson, H., and Matthews, B. W. (1991) *Biochemistry 30*, 7142−7153.
31. Dill, K. A. (1990) *Biochemistry 29*, 7133−7155.
32. Malakauskas, S. M., and Mayo, S. L. (1998) *Nat. Struct. Biol. 5*, 470−475.
33. Koide, A., Jordan, M. R., Horner, S. R., Batori, V., and Koide, S. (2001) *Biochemistry 40*, 10326−10333.
34. Muzammil, S., Kumar, Y., and Tayyab, S. (2000) *Proteins 40*, 29−38.
35. Shortle, D., and Ackerman, M. S. (2001) *Science 293*, 487−489.
36. Chehin, R., Iloro, I., Marcos, M. J., Villar, E., Shnyrov, V. L., and Arrondo, J. L. R. (1999) *Biochemistry 38*, 1525−1530.
37. Schwarzbauer, J. E., and Sechler, J. L. (1999) *Curr. Opin. Cell Biol. 11*, 622−627.
38. Ohashi, T., Kiehart, D. P., and Erickson, H. P. (1999) *Proc. Natl. Acad. Sci. U.S.A. 96*, 2153−2158.
39. Craig, D., Krammer, A., Schulten, K., and Vogel, V. (2001) *Proc. Natl. Acad. Sci. U.S.A. 98*, 1351−1356.
40. Altroff, H., Choulier, L., and Mardon, H. J. (2003) *J. Biol. Chem. 278*, 491−497.
41. Baneyx, G., Baugh, L., and Vogel, V. (2001) *Proc. Natl. Acad. Sci. U.S.A. 98*, 14464−14468.
42. Baneyx, G., Baugh, L., and Vogel, V. (2002) *Proc. Natl. Acad. Sci. U.S.A. 99*, 5139−5143.

BI0347104